

---

# AUTOMATIC WHITE MATTER HYPERINTENSITY PARCELLATION: T1W BRAIN ATLAS AND CORRESPONDING SOFTWARE

---

**Ben Philps**  
School of Informatics  
University of Edinburgh  
Edinburgh, UK  
s2208943@ed.ac.uk

**Maria del C. Valdes Hernandez**  
Centre for Clinical Brain Sciences  
University of Edinburgh  
Edinburgh, UK  
M.Valdes-Hernan@ed.ac.uk

**Miguel O. Bernabeu**  
Usher Institute  
University of Edinburgh  
Edinburgh, UK  
miguel.bernabeu@ed.ac.uk

September 26, 2025

## Abbreviations

- WMH - White Matter Hyperintensities
- BGIT - Combined Basal Ganglia, Inter-lobe and Thalamus region
- MRI - Magnetic Resonance Imaging
- ROI - Region of Interest
- ICV - Intracranial Volume

## 1 Summary

White matter hyperintensities (WMH) are one of the core pathognomonic correlates of cerebral small vessel disease visible in brain MRI. Here we provide a T1w brain MRI atlas and software for parcellating a given WMH segmentation into 36 anatomical regions of interest (ROI) following the previously established bullseye parcellation of WMH [1] (which effectively captures all visual rating scales for WMH). This technique first divides white matter into 4 equidistant concentric layers extending from the ventricles to the cortex. Secondly, frontal, parietal, temporal and occipital lobes are delineated for both hemispheres of the brain, while the basal ganglia, thalamus and inter-lobe regions are combined (known as the BGIT region). We provide a brain atlas template for obtaining the lobar segmentation via registration, along with software to construct the concentric layers using output from the SynthSeg[2] tool. This tool allows for a rapid and robust registration based parcellation. We do not provide a WMH segmentation tool here, instead our parcellation tool may be used in conjunction with any WMH segmentation algorithm, or for parcellating any other ROI into the same anatomical regions of interest. For the latest version of our pipeline, see <https://github.com/BenjaminPhi5/auto-wmh-bullseye-parc>.

## 2 Dataset Description

We provide a z-score normalized copy of a 73 year old average brain template which should be used for registration to the subject image under study. To register to subject images that have not been z-score normalized, please download the original 73 year old template image from Edinburgh Datashare at <https://doi.org/10.7488/ds/1369>. We also provide a brain atlas for the lobe parcellation both with and without the BGIT region. We also provide the output of SynthSeg for the template image (although this is not required for the parcellation). All images are provided as NIFTI files. We provide code for computing the bullseye parcellation in subject image space. Finally, we provide csv files that provide the names of each ROI in the lobe atlas and final WMH parcellation. In section 4 we provide instructions for conducting the parcellation, while section 5 provides an extended discussion of the automated bullseye parcellation. **Note:** our software presumes all images used for parcellation, including WMH segmentations, are provided in NIFTI format.

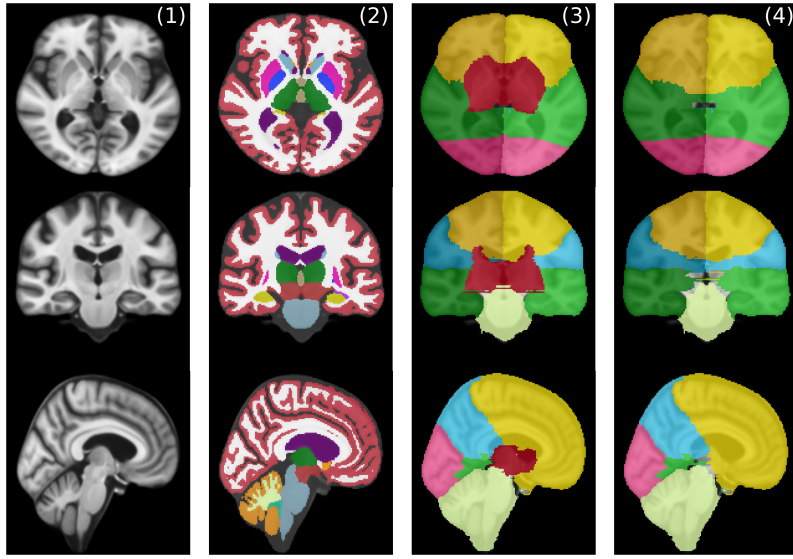


**Figure (1) Brain template and corresponding lobe atlas.** (1) T1w template image. (2) SynthSeg anatomical segmentation. (3) Manually corrected brain lobe atlas. Regions of interest shown are frontal (orange), parietal (blue), temporal (green), occipital (pink), BGIT (red), brainstem/cerebellum (beige). (3): The brain atlas, excluding the BGIT region, where BGIT voxels are assigned to one of the four lobes.

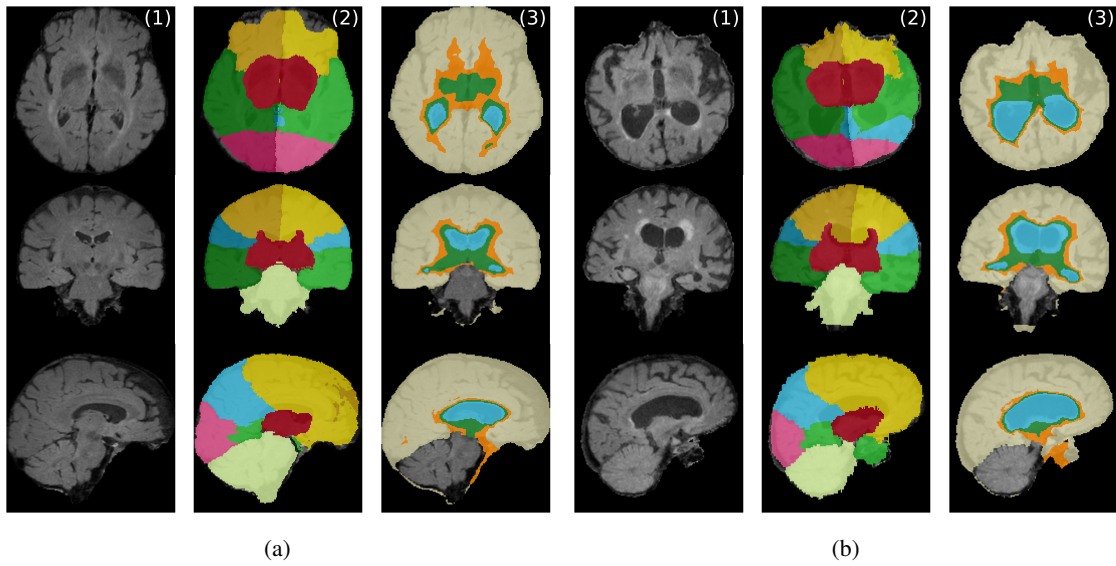


**Figure (2) Examples of the lobe atlas registered to the space of a subject image, and the ventricle to cortex layers, which combine to construct the bullseye parcellation.** (a) A 77 year old subject with limited WMH. (b) A 74 year old subject with ventricular expansion and substantial WMH. (1) FLAIR MRI. (2) Lobe atlas transformed to the subject space. (3) Layers 1 to 4 of the bullseye parcellation, dividing the distance from the ventricles to the cortex into 4 equidistant layers. Subject images were obtained from the Australian Imaging Biomarkers and Lifestyle flagship study of ageing (AIBL) [3]. See [www.aibl.csiro.au](http://www.aibl.csiro.au) for further details.

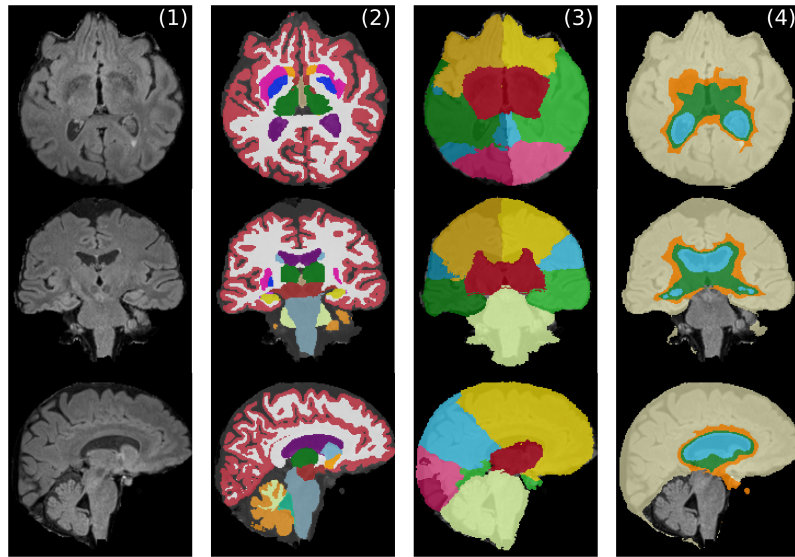


**Figure (3) Automated bullseye parcellation may introduce registration errors or confuse periventricular and deep WMH.** (1) FLAIR image of a subject (66 years old) with visible WMH at the right occipital/temporal horn, taken from the AIBL dataset [3]. (2) Anatomical segmentation used to calculate the layers of the bullseye parcellation. (3) Lobe atlas transformed to the subject space. Registration errors can result in assymetric ROI in the resulting bullseye parcellation, with the parietal lobe visible in only the left hemisphere (top row - blue) or uneven overlap between hemispheres seen in the occipital lobe (bottom row - pink). (4) Layers 1 to 4 of the bullseye parcellation. Due to the proximity to the cortex (see red segmentation label in (2)), the WMH below the ventricle horns (top row, right hemisphere) that may typically be classified as periventricular WMH (e.g. in the Fazekas visual rating scale) are assigned to ring 4 in the bullseye parcellation.

### 3 Datset Contents

- `atlas_bgit.nii.gz` - the manually delineated lobes (frontal, parietal, temporal, occipital) and the BGIT region.
- `atlas_no_bgit.nii.gz` - the manually delineated lobes without the BGIT region.
- `template_73y_stripped.nii.gz` - the template image after applying skull stripping. This image should be used for the registration if the subject image has already been skull-stripped (but not normalized).
- `template_73y_normalized.nii.gz` - the template image after applying skull stripping and z-score normalization. This image should be used for the registration if the subject image has already been skull-stripped and normalized.
- `template_73y_synthseg.nii.gz` - the output of Synthseg in the template space. This can be used to calculate the location of the anatomical regions of interest in the subject space by applying the registration transform from the registration step to this image, however, directly computing the segmentation in the subject space is preferred.
- `template_73y_synthstripmask.nii.gz` - the brainmask (ICV) of template image, used during registration.
- `WMH-parcellation-labels.csv` - this spreadsheet provides the name of each ROI provided by the WMH parcellation code.
- `WMH-LobeAtlas-labels.csv` - this spreadsheet provides the name of each label in the `atlas_bgit.nii.gz` and `atlas_no_bgit.nii.gz` files.
- `code.zip` - the software for computing the WMH parcellation.

### 4 WMH Parcellation Instructions

To perform the WMH Parcellation you will need a anatomical MRI `subject_img.nii.gz`, brainmask (ICV file) `subject_icv.nii.gz` and a WMH segmentation `subject_wmh.nii.gz`.

## 4.1 Installation

We make use FreeSurfer tools for image resampling, and the SynthSeg tool (installation instructions for FreeSurfer can be found here: <https://surfer.nmr.mgh.harvard.edu/fswiki/DownloadAndInstall>). Alternatively, SynthSeg can be installed in a python environment (see instructions here: <https://github.com/BBillot/SynthSeg>). We also presume Miniconda is installed for creating conda environments (however, any other python environment manager of your preference is fine). To install miniconda, see instructions here <https://www.anaconda.com/docs/getting-started/miniconda/main>.

To install our WMH parcellation code, first either clone the repository with `git clone git@github.com:BenjaminPhi5/auto-wmh-bullseye-parc.git` or unzip the provided `code.zip` file. To install the WMH parcellation code repository, follow these steps:

```
cd auto-wmh-bullseye-parc
conda create -y --name wmhparc python=3.12.8
conda activate wmhparc
pip install -e .
```

## 4.2 Step 1 - Run SynthSeg

Once FreeSurfer is installed you can run SynthSeg with the following command:

```
mri_synthseg --i <input> --o <output> --cpu 12
```

Please see <https://surfer.nmr.mgh.harvard.edu/fswiki/SynthSeg> for an explanation of the arguments. We recommend using the `-cpu` command with as many cpu cores as available to you.

## 4.3 Step 2 - Compute Parcellation

Run our WMH parcellation pipeline with the following command

```
conda activate wmhparc
python wmhparc/run_parcellation.py \
--image subject_img.nii.gz \
--brainmask subject_icv.nii.gz \
--synthseg subject_synthseg.nii.gz \
--template <path to template, e.g template_73y_normalized.nii.gz> \
--atlas <path to atlas_bgit.nii.gz> \
--wmh_seg subject_wmh.nii.gz \
--output_folder <desired output folder>
```

In the desired output folder, this script will create files ending in the following:

- `bullseye_parc_wmh_vols.csv` : A spreadsheet providing the volume in mm<sup>3</sup> of WMH in each ROI of the bullseye parcellation.
- `bullseye_parc.nii.gz` : The bullseye parcellation segmentation file, with labels corresponding to WMH-parcellation-labels.csv.
- `pvrings.nii.gz` : The concentric layers of the bullseye parcellation, with labels 1-4 representing layers 1-4.
- `lobe_atlas.nii.gz` : The lobes and BGIT regions of the bullseye parcellation with labels corresponding to WMH-LobeAtlas-labels.csv
- `lobe_atlas_template_synaggro_0GenericAffine.mat` : The affine component of the registration transform between the template image and subject anatomical image provided by ANTS.
- `lobe_atlas_template_synaggro_1Warp.nii.gz` : The non-linear component of the registration transform provided by ANTS.
- `lobe_atlas_template_synaggro_1InverseWarp.nii.gz` : The inverse of the non-linear component of the registration provided by ANTS.
- `cortexdist.nii.gz` : The Euclidean distance between all voxels and the cortex.
- `ventdist.nii.gz` : The Euclidean distance between all voxels and the lateral ventricles.

## 5 Background and Methods

### 5.1 Brain Parcellation

Parcellation is the process of dividing the human brain into regions or ‘parcels’, typically depending on anatomical structure, function or connectivity - yielding a low dimensional representation of the large-scale functional networks of the brain, facilitating further analysis. Given the functional separation and long range connections between spatial regions of the brain, parcellation is key to understanding the brain [4]. A range of parcellation techniques have been proposed [5], frequently utilizing functional [6] and diffusion MRI [7] to determine parcels based on functional or connectivity characteristics. Parcellation is widely utilized for understanding brain organization [8, 9, 10] and for identifying differences between subjects with different characteristics (e.g cognition, disease subtype or age) [11, 9, 12, 10, 13], trajectories of neurodegenerative diseases [14, 15, 16] or psychopathology [17, 18].

Due to the lack of anatomical landmarks for classifying white matter, automatic white matter parcellation typically relies on either extrapolating from a gray matter parcellation (as performed in FreeSurfer[19]) or registration [20]. A number of white matter parcellation atlases have been created [21, 7, 22]. However analysis of WMH typically utilizes visual rating scales [23, 24], with inherently large parcels. Furthermore, registration of templates to subjects with atrophy or WMH present can lead to registration errors [25], impacting the parcellation [26]. Registration errors are particularly problematic when parcels are small [27], hence choosing the right level of granularity for analysis remains a challenge.

### 5.2 The WMH Bullseye Parcellation

The bullseye parcellation proposed by Sudre et al. [1] provides a patient specific division of the brain for parcellating automated segmentations of WMH, and bridges the gap between fine-grained connectivity derived white matter parcellations and the coarse visual scales typical of WMH analysis. The parcellation divides the brain into 36 distinct parcels by intersecting lobar boundaries with distance boundaries between the ventricles and cortex. This technique first divides white matter into 4 equidistant concentric layers extending from the ventricles to the cortex. These layers can be calculated at the voxel level using euclidian distance transforms from each voxel to the cortical gray matter and ventricle surfaces. This relative distance is calculated individually per patient, accounting for subject atrophy levels. Secondly, frontal, parietal, temporal and occipital lobes are delineated for both hemispheres of the brain, while the basal ganglia, thalamus and inter-lobe regions are combined (known as the BGIT region). Combining these 9 lobe regions (4 lobes in 2 hemispheres plus the interlobe region) and 4 layers from the ventricles to the cortex gives a parcellation of 36 ROI. The bullseye parcellation can represent a wide range of established visual rating scales [1] for WMH, addresses the inter-rater variability inherent to visual rating scales [28, 24, 29, 23] and has been deployed in a wide range of studies to study the relationship between spatial WMH characteristics and cognition [30, 31], amyloid pathology [32], dementia risk factors [33] and Wilson’s disease [34].

Previous works using the bullseye parcellation typically utilize FreeSurfer[35] or the Geodesic Information Flow (GIF) label fusion tool [36] for anatomical segmentation and cortical gray matter parcellation, after which lobar boundaries are calculated by propagating the cortical parcellation labels to the white matter. However, performing parcellation of each subject is slow and leads to erroneous and inconsistent lobar and ventricle boundaries, complicating large-scale analysis. Instead, we developed a lobe atlas on an age appropriate template that assigns every voxel in the brain to one of the frontal, parietal, temporal, occipital or BGIT regions (excluding the brainstem and cerebellum). This atlas is applied to every subject image via registration. Due to assigning every voxel to a label and the large size of the lobe labels, the impact of registration errors, particularly in matching the ventricles, is minimized. To calculate the concentric layers of the bullseye parcellation we first require a segmentation of the ventricles and cortex. We extract these using SynthSeg[2], a fast neural network tool for anatomical segmentation with high inter-scanner and test-retest reliability [37], making it suitable for large-scale heterogenous cohort analysis. Figure 1 demonstrates the brain lobe atlas, while Figure 2 demonstrates the lobe and layer components of the bullseye on two example subjects.

### 5.3 Developing a Brain Lobe Atlas

This section outlines the development of the brain lobe atlas image used as part of the automated bullseye parcellation pipeline.

Our goal is to analyse large scale cognitively normal and dementia subjects. Given the manual editing required to generate an accurate lobe atlas, we ideally wish to choose to use a single template and corresponding atlas across all subjects. During initial experimentation, we found that elderly templates from cognitively normal and dementia groups yielded comparable registration performance across a range of disease cohorts while younger healthy templates

introduced more errors. hence we selected an age appropriate template (a cognitively normal average T1w template image derived from 47 subjects aged 71-74 years [38]).

Our lobe atlas is developed in a semi-automated manner. First, cortical reconstruction and volumetric segmentation was performed with the FreeSurfer image analysis pipeline [35] (<http://surfer.nmr.mgh.harvard.edu/>) The cortex is parcellated using the Desikan-Killany atlas [39, 40]. FreeSurfer automatically assigns gyral white matter within 5mm of the cortex to the label matching the nearest cortical parcellation label [19]. White matter parcels are then grouped into the frontal, parietal, temporal and occipital lobes. However, white matter outside the juxtacortical region are not assigned to a region. To assign deep and periventricular white matter regions to a lobe, we first dilate each lobe label mask (strictly within the white matter voxels). Specifically, white matter voxels with a euclidian distance  $< 5\text{mm}^3$  of any of the lobes are assigned to the lobe for which the voxel to lobe-mask distance is smallest. After which, the remaining white matter within the centrum semiovale is assigned to the inter-lobe (BGIT) region, along with the basal ganglia and thalamus structures. All remaining voxels within the brain-mask that have not been assigned to one of the four lobes, BGIT region, brainstem or cerebellum are assigned to the lobe with the smallest euclidian distance. Annotations for the brainstem or cerebellum are taken from the anatomical segmentation from the FreeSurfer pipeline.

Second, once the initial automated lobe segmentation was complete, the atlas was extensively manually edited to correct errors around the true lobe boundaries and those obtained via manipulation of the FreeSurfer parcellation, resulting in the final brain atlas. Furthermore, voxels assigned to the four lobes in the final voxel assignment step which belong to other structures were manually corrected.

#### 5.4 Calculating the WMH parcellation on a new subject image

In this section we outline the procedure to generate the WMH parcellation for a given subject image. However, users are of course free to use the provided atlas as they wish.

##### 5.4.1 Prerequisites

To conduct this procedure we assume that an anatomical image (e.g T1w or FLAIR MRI), WMH segmentation mask and a brainmask (ICV file) are provided. As the brain template is skull stripped, the anatomical image should be skull stripped before registration. If the template is not skull stripped, we recommend the SynthStrip tool [41] for skull stripping. If your image is has been z-score normalized, then we provide a z-score normalized variant of the image template `template_73y_normalized.nii.gz` that should be used in the steps below. Otherwise the original template should be used, which can be downloaded from Edinburgh Datashare at <https://doi.org/10.7488/ds/1369> (please download the 73 year old template brain).

##### 5.4.2 Registration

To determine the lobe segmentations in the subject image space, we register the brain template to the subject anatomical image. We first apply a linear affine transformation (12 degrees of freedom), followed by a deformable transformation (Symmetric normalization algorithm [42]), with the Mattes mutual information metric for both steps. We use the ANTS registration toolkit[43, 44] to perform registration. The resulting registration transforms are then applied to the brain lobe atlas (`atlas_bgkit.nii.gz`) using nearest neighbour interpolation.

##### 5.4.3 Bullseye layers computation

After applying SynthSeg[2] to the anatomical subject image, we then compute two distance transforms, one representing the distance from each voxel to the ventricles and the other the distance to the cortex. The normalized distance between the two regions is then calculated as:

$$\frac{\text{Distance to ventricles}_v}{\text{Distance to ventricles}_v + \text{Distance to cortex}_v}, \quad (1)$$

where  $v$  is the voxel index. This distance map is discretized into four layers corresponding to the boundaries: [0, 0.25), [0.25, 0.5), [0.5, 0.75), [0.75, 1], where the first layer corresponds to voxels closest to the ventricles and the fourth the voxels closest to the cortex. The final subject specific WMH parcellation map is calculated by taking the intersection of the layer and lobe maps. Voxels outside the brainmask are excluded.

We also provide the anatomical segmentation (SynthSeg output) for the template, so users can forgo computing an anatomical segmentation and instead apply the registration transforms to the template space segmentation. However to reduce the impact of registration errors around the ventricles and cortex which will impact the calculation of the

bullseye layers, we highly recommend users use a tool such as SynthSeg to calculate anatomical segmentations directly in subject space.

### 5.5 Limitations

Our parcellation procedure is limited to a single brain atlas template. A formal analysis of the sensitivity of the resulting WMH parcellation atlas to the choice of template (e.g. using publicly available and disease appropriate templates [45]) is warranted to further validate our approach. Nonetheless, any advantage in selecting a different template (e.g. more accurate registration) comes with the cost of requiring re-annotation of the brain lobe atlas.

A fully automated pipeline for WMH parcellation will always risk introducing unusual parcellations in some cases. For example, where cortical foldings come close to the ventricles, WMH that are typically considered periventricular may be classified in the outer layers (3 and 4) of the bullseye parcellation. Furthermore, registration based annotation lobes can introduce some confusion between lobes and hemispheres see Figure 3.

The bullseye provides 36 ROI for analysis, however many of these are highly co-linear, complicating downstream analysis. A number of works have further reduced the bullseye parcellation to a handful of principle components for simplified analysis [30, 33, 31]. However, no unified principle components and corresponding linear weights in the original bullseye parcellation have been provided. Given our fully automated approach, this is something we could develop, using large-scale cohort analysis, but this remains for future work.

Here we have focussed on the bullseye parcellation specifically. However the formulation of the bullseye parcellation is primarily driven by unifying visual rating scales for WMH assessment, not underlying neural architecture and function. Further work should explore whether tract based diffusion imaging derived atlas techniques for white matter parcellation can be effectively ported WMH parcellation. This may better allow us to study the relationship between WMH and functional outcomes in a large-scale, automated manner.

## 6 Funding

B.P. is funded by the United Kingdom Research and Innovation Centre for Doctoral Training in Biomedical AI Programme scholarships (grant EP/S02431X/1). M.V.H. is funded by The Row Fogo Charitable Trust (Grant No. BROD.FID3668413). M.O.B. gratefully acknowledges funding from: Fondation Leducq Transatlantic Network of Excellence (17 CVD 03); EPSRC grant no. EP/X025705/1; British Heart Foundation and The Alan Turing Institute Cardiovascular Data Science Award (C-10180357); Diabetes UK (20/0006221); Fight for Sight (5137/5138); the SCONE projects funded by Chief Scientist Office, Edinburgh & Lothians Health Foundation, Sight Scotland, the Royal College of Surgeons of Edinburgh, the RS Macdonald Charitable Trust, and Fight For Sight; the Neurii initiative which is a partnership among Eisai Co., Ltd, Gates Ventures, LifeArc and HDR UK.

## References

- [1] Carol H Sudre, B Gomez Anson, Indran Davagnanam, A Schmitt, Alex F Mendelson, F Prados, Lorna Smith, David Atkinson, Alun D Hughes, N Chaturvedi, et al. Bullseye's representation of cerebral white matter hyperintensities. *Journal of Neuroradiology*, 45(2):114–122, 2018.
- [2] Benjamin Billot, Douglas N Greve, Oula Puonti, Axel Thielscher, Koen Van Leemput, Bruce Fischl, Adrian V Dalca, Juan Eugenio Iglesias, et al. Synthseg: Segmentation of brain mri scans of any contrast and resolution without retraining. *Medical image analysis*, 86:102789, 2023.
- [3] Kathryn A Ellis, Ashley I Bush, David Darby, Daniela De Fazio, Jonathan Foster, Peter Hudson, Nicola T Lautenschlager, Nat Lenzo, Ralph N Martins, Paul Maruff, et al. The australian imaging, biomarkers and lifestyle (aibl) study of aging: methodology and baseline characteristics of 1112 individuals recruited for a longitudinal study of alzheimer's disease. *International psychogeriatrics*, 21(4):672–687, 2009.
- [4] Simon B Eickhoff, BT Thomas Yeo, and Sarah Genon. Imaging-based parcellations of the human brain. *Nature Reviews Neuroscience*, 19(11):672–686, 2018.
- [5] Salim Arslan, Sofia Ira Ktena, Antonios Makropoulos, Emma C Robinson, Daniel Rueckert, and Sarah Parisot. Human brain mapping: A systematic comparison of parcellation methods for the human cerebral cortex. *NeuroImage*, 170:5–30, 2018.
- [6] Pantea Moghimi, Anh The Dang, Quan Do, Theoden I Netoff, Kelvin O Lim, and Gowtham Atluri. Evaluation of functional mri-based human brain parcellation: a review. *Journal of neurophysiology*, 128(1):197–217, 2022.

- [7] Ahmed M Radwan, Stefan Sunaert, Kurt Schilling, Maxime Descoteaux, Bennett A Landman, Mathieu Vandebulcke, Tom Theys, Patrick Dupont, and Louise Emsell. An atlas of white matter anatomy, its variability, and reproducibility based on constrained spherical deconvolution of diffusion mri. *NeuroImage*, 254:119029, 2022.
- [8] Lingzhong Fan, Hai Li, Junjie Zhuo, Yu Zhang, Jiaojian Wang, Liangfu Chen, Zhengyi Yang, Congying Chu, Sangma Xie, Angela R Laird, et al. The human brainnetome atlas: a new brain atlas based on connectional architecture. *Cerebral cortex*, 26(8):3508–3526, 2016.
- [9] NV Bryce, JC Flournoy, JFG Moreira, ML Rosen, KA Sambook, P Mair, and KA McLaughlin. Brain parcellation selection: An overlooked decision point with meaningful effects on individual differences in resting-state functional connectivity. *neuroimage*, 243, article 118487, 2021.
- [10] Renaud Lopes, Christine Delmaire, Luc Defebvre, Anja J Moonen, Annelien A Duits, Paul Hofman, Albert FG Leentjens, and Kathy Dujardin. Cognitive phenotypes in parkinson’s disease differ in terms of brain-network organization and connectivity. *Human brain mapping*, 38(3):1604–1621, 2017.
- [11] Katherine C Lopez, Sridhar Kandala, Scott Marek, and Deanna M Barch. Development of network topology and functional connectivity of the prefrontal cortex. *Cerebral Cortex*, 30(4):2489–2505, 2020.
- [12] Anna Plachti, Shahrzad Kharabian, Simon B Eickhoff, Somayeh Maleki Balajoo, Felix Hoffstaedter, Deepthi P Varikuti, Christiane Jockwitz, Svenja Caspers, Katrin Amunts, and Sarah Genon. Hippocampus co-atrophy pattern in dementia deviates from covariance patterns across the lifespan. *Brain*, 143(9):2788–2802, 2020.
- [13] Christine C Guo, Rachel Tan, John R Hodges, Xintao Hu, Saber Sami, and Michael Hornberger. Network-selective vulnerability of the human cerebellum to alzheimer’s disease and frontotemporal dementia. *Brain*, 139(5):1527–1538, 2016.
- [14] Zhijian Yang, Ilya M Nasrallah, Haochang Shou, Junhao Wen, Jimit Doshi, Mohamad Habes, Guray Erus, Ahmed Abdulkadir, Susan M Resnick, Marilyn S Albert, et al. A deep learning framework identifies dimensional representations of alzheimer’s disease from brain structure. *Nature communications*, 12(1):7065, 2021.
- [15] Zhanxiong Wu, Dong Xu, Thomas Potter, Yingchun Zhang, and Alzheimer’s Disease Neuroimaging Initiative. Effects of brain parcellation on the characterization of topological deterioration in alzheimer’s disease. *Frontiers in aging neuroscience*, 11:113, 2019.
- [16] Liwen Zhang, Elijah Mak, Anthonin Reilhac, Hee Y Shim, Kwun K Ng, Marcus QW Ong, Fang Ji, Eddie JY Chong, Xin Xu, Zi X Wong, et al. Longitudinal trajectory of amyloid-related hippocampal subfield atrophy in nondemented elderly. *Human brain mapping*, 41(8):2037–2047, 2020.
- [17] Lena KL Oestreich, Roshini Randeniya, and Marta I Garrido. White matter connectivity reductions in the pre-clinical continuum of psychosis: A connectome study. *Human brain mapping*, 40(2):529–537, 2019.
- [18] Nicco Reggente, Teena D Moody, Francesca Morfini, Courtney Sheen, Jesse Rissman, Joseph O’Neill, and Jamie D Feusner. Multivariate resting-state functional connectivity predicts response to cognitive behavioral therapy in obsessive-compulsive disorder. *Proceedings of the National Academy of Sciences*, 115(9):2222–2227, 2018.
- [19] David H Salat, Douglas N Greve, Jennifer L Pacheco, Brian T Quinn, Karl G Helmer, Randy L Buckner, and Bruce Fischl. Regional white matter volume differences in nondemented aging and alzheimer’s disease. *NeuroImage*, 44(4):1247–1258, 2009.
- [20] Patrick Schiffler, Jan-Gerd Tenberge, Heinz Wiendl, and Sven G Meuth. Cortex parcellation associated whole white matter parcellation in individual subjects. *Frontiers in human neuroscience*, 11:352, 2017.
- [21] Kenichi Oishi, Karl Zilles, Katrin Amunts, Andreia Faria, Hangyi Jiang, Xin Li, Kazi Akhter, Kegang Hua, Roger Woods, Arthur W Toga, et al. Human brain white matter atlas: identification and assignment of common anatomical structures in superficial white matter. *NeuroImage*, 43(3):447–457, 2008.
- [22] Luke Bloy, Madhura Ingalkar, Harini Eavani, Robert T Schultz, Timothy PL Roberts, and Ragini Verma. White matter atlas generation using hardi based automated parcellation. *NeuroImage*, 59(4):4055–4063, 2012.
- [23] Alida A Gouw, Wiesje Maria van der Flier, Elisabeth CW van Straaten, Leonardo Pantoni, Antonio J Bastos-Leite, Domenico Inzitari, Timo Erkinjuntti, Lars-Olof Wahlund, C Ryberg, Reinhold Schmidt, et al. Reliability and sensitivity of visual scales versus volumetry for evaluating white matter hyperintensity progression. *Cerebrovascular diseases*, 25(3):247–253, 2008.
- [24] KS King, Ronald M Peshock, MW Warren, L Alhilali, K Hulsey, R McColl, MF Weiner, C Ayers, and A Whittemore. Evaluation of a practical visual mri rating scale of brain white matter hyperintensities for clinicians based on largest lesion size regardless of location. *American Journal of Neuroradiology*, 34(4):797–801, 2013.

- [25] Mahsa Dadar, Vladimir S Fonov, D Louis Collins, Alzheimer's Disease Neuroimaging Initiative, et al. A comparison of publicly available linear mri stereotaxic registration techniques. *Neuroimage*, 174:191–200, 2018.
- [26] Torsten Rohlfing. Incorrect icbm-dti-81 atlas orientation and white matter labels, 2013.
- [27] Ross M Lawrence, Eric W Bridgeford, Patrick E Myers, Ganesh C Arvapalli, Sandhya C Ramachandran, Derek A Pisner, Paige F Frank, Allison D Lemmer, Aki Nikolaidis, and Joshua T Vogelstein. Standardizing human brain parcellations. *Scientific data*, 8(1):78, 2021.
- [28] Aoife M Haughey, Roisin M O'Cearbhail, Stephanie Forté, Joanna D Schaafsma, Kevin HM Kuo, and Igor Gomes Padilha. Assessment of inter-reader reliability of fazekas scoring on magnetic resonance imaging of the brain in adult patients with sickle cell disease. *Diagnostics*, 15(7):857, 2025.
- [29] P Kapeller, R Barber, RJ Vermeulen, H Ader, P Scheltens, W Freidl, O Almkvist, M Moretti, T Del Ser, P Vaghfeldt, et al. Visual rating of age-related white matter changes on magnetic resonance imaging: scale comparison, interrater agreement, and correlations with quantitative measurements. *Stroke*, 34(2):441–445, 2003.
- [30] Joan Jiménez-Balado, Fabian Corlier, Christian Habeck, Yaakov Stern, and Teal Eich. Effects of white matter hyperintensities distribution and clustering on late-life cognitive impairment. *Scientific reports*, 12(1):1955, 2022.
- [31] Dario Bachmann, Bettina von Rickenbach, Andreas Buchmann, Martin Hüllner, Isabelle Zuber, Sandro Studer, Antje Saake, Katrin Rauen, Esmeralda Gruber, Roger M Nitsch, et al. White matter hyperintensity patterns: associations with comorbidities, amyloid, and cognition. *Alzheimer's Research & Therapy*, 16(1):67, 2024.
- [32] Lene Pålhaugen, Carole H Sudre, Sandra Tecelao, Arne Nakling, Ina S Almdahl, Lisa F Kalheim, M Jorge Cardoso, Stein H Johnsen, Arvid Rongve, Dag Aarsland, et al. Brain amyloid and vascular risk are related to distinct white matter hyperintensity patterns. *Journal of Cerebral Blood Flow & Metabolism*, 41(5):1162–1174, 2021.
- [33] Frauke Beyer, Ami Tsuchida, Aicha Soumaré, Hema Sekhar Reddy Rajula, Aniket Mishra, Fabrice Crivello, Cécile Proust-Lima, Markus Loeffler, Christophe Tzourio, Philippe Amouyel, et al. White matter hyperintensity spatial patterns: Risk factors and clinical correlates. *Alzheimer's & Dementia*, 21(4):e70053, 2025.
- [34] Samuel Shribman, Martina Bocchetta, Carole H Sudre, Julio Acosta-Cabronero, Maggie Burrows, Paul Cook, David L Thomas, Godfrey T Gillett, Emmanuel A Tsochatzis, Oliver Bandmann, et al. Neuroimaging correlates of brain injury in wilson's disease: a multimodal, whole-brain mri study. *Brain*, 145(1):263–275, 2022.
- [35] Bruce Fischl. Freesurfer. *Neuroimage*, 62(2):774–781, 2012.
- [36] M Jorge Cardoso, Marc Modat, Robin Wolz, Andrew Melbourne, David Cash, Daniel Rueckert, and Sébastien Ourselin. Geodesic information flows: spatially-variant graphs and their application to segmentation and fusion. *IEEE transactions on medical imaging*, 34(9):1976–1988, 2015.
- [37] David R Van Nederpelt, Houshang Amiri, Iman Brouwer, Samantha Noteboom, Lidwine B Mokkink, Frederik Barkhof, Hugo Vrenken, and Joost PA Kuijjer. Reliability of brain atrophy measurements in multiple sclerosis using mri: an assessment of six freely available software packages for cross-sectional analyses. *Neuroradiology*, 65(10):1459–1472, 2023.
- [38] DA Dickie, DE Job, D Rodriguez, A Robson, S Danso, C Pernet, ME Bastin, IJ Deary, SD Shenkin, and JM Wardlaw. Brain imaging of normal subjects (brains) age-specific mri atlases from young adults to the very elderly (v1. 0),[dataset]. *University of Edinburgh, Edinburgh Imaging, CCBS, BRAINS Imagebank*. doi, 10:7488, 2016.
- [39] Rahul S Desikan, Florent Ségonne, Bruce Fischl, Brian T Quinn, Bradford C Dickerson, Deborah Blacker, Randy L Buckner, Anders M Dale, R Paul Maguire, Bradley T Hyman, et al. An automated labeling system for subdividing the human cerebral cortex on mri scans into gyral based regions of interest. *Neuroimage*, 31(3):968–980, 2006.
- [40] Bruce Fischl, André Van Der Kouwe, Christophe Destrieux, Eric Halgren, Florent Ségonne, David H Salat, Evelina Busa, Larry J Seidman, Jill Goldstein, David Kennedy, et al. Automatically parcellating the human cerebral cortex. *Cerebral cortex*, 14(1):11–22, 2004.
- [41] Andrew Hoopes, Jocelyn S Mora, Adrian V Dalca, Bruce Fischl, and Malte Hoffmann. Synthstrip: skull-stripping for any brain image. *NeuroImage*, 260:119474, 2022.
- [42] Brian B Avants, Charles L Epstein, Murray Grossman, and James C Gee. Symmetric diffeomorphic image registration with cross-correlation: evaluating automated labeling of elderly and neurodegenerative brain. *Medical image analysis*, 12(1):26–41, 2008.
- [43] Brian B Avants, Nicholas J Tustison, Gang Song, Philip A Cook, Arno Klein, and James C Gee. A reproducible evaluation of ants similarity metric performance in brain image registration. *Neuroimage*, 54(3):2033–2044, 2011.

- [44] Brian B Avants, Nicholas J Tustison, Michael Stauffer, Gang Song, Baohua Wu, and James C Gee. The insight toolkit image registration framework. *Frontiers in neuroinformatics*, 8:44, 2014.
- [45] Mahsa Dadar, Richard Camicioli, and Simon Duchesne. Multi sequence average templates for aging and neurodegenerative disease populations. *Scientific Data*, 9(1):238, 2022.